Transport and Stability of High-β_N, High Noninductive Fraction DIII-D Discharges

F. Turco[1], T.C. Luce[2], J.R. Ferron[2], C.T. Holcomb[3], D.P. Brennan[4], J.C. DeBoo[2], A.E. White[5], P.A. Politzer[2], and Y. In[6]

[1]*Oak Ridge Associated Universities, PO Box 117, Oak Ridge, TN 37831-0117, USA*
[2]*General Atomics, PO Box 85608, San Diego, CA 92186-5608, USA*
[3]*Lawrence Livermore National Laboratory, 700 East Ave., Livermore, CA 94550, USA*
[4]*University of Tulsa, 800 S. Tucker Dr., Tulsa, OK 74104, USA*
[5]*Massachusetts Institute of Technology, 77 Massachusetts Ave., Cambridge, MA 02139, USA*
[6]*FAR-TECH, Inc., 10350 Science Center Dr., Bldg 14, Suite 150, San Diego, CA 92121, USA*

Introduction

In order to create a scenario with high fusion gain and 100% noninductive current, a large fraction of the current must be sustained by bootstrap current (J_{BS}). Under these conditions, the normalised ratio of plasma to magnetic pressure (β_N) also has to be large, and the magnitude and location of J_{BS} are nonlinearly coupled with the evolution of the safety factor profile (q), because of the feedback loop existing between q, transport and the kinetic profiles. Therefore, understanding the dependence of transport on the q profile in this regime is critical to the optimization. Moreover, high-performance, high noninductive current fraction plasmas are often limited by n=1 tearing modes, that deteriorate the confinement and modify the current profile in a way that is not recoverable with the available current sources. For these reasons, experiments were conducted in the DIII-D tokamak, using systematic scans of q_{min} and q_{95}, at both fixed and maximum β_N, in order to determine empirically the variation of the transport properties with q, and the best alignment of the noninductive currents with the total current profile.

ECCD influences the tearing stability

Electron cyclotron (EC) current is one of the sources used to provide part of the noninductive current required in excess of the bootstrap current. Experiments have shown that it has a positive influence on the tearing stability of the discharges, if aimed with a broad deposition at mid radius. Time traces from a model discharge are plotted in figure 1. The black traces show the stable discharge, while the red and the blue traces (with the same EC deposition location and profile) show that modes become unstable shortly

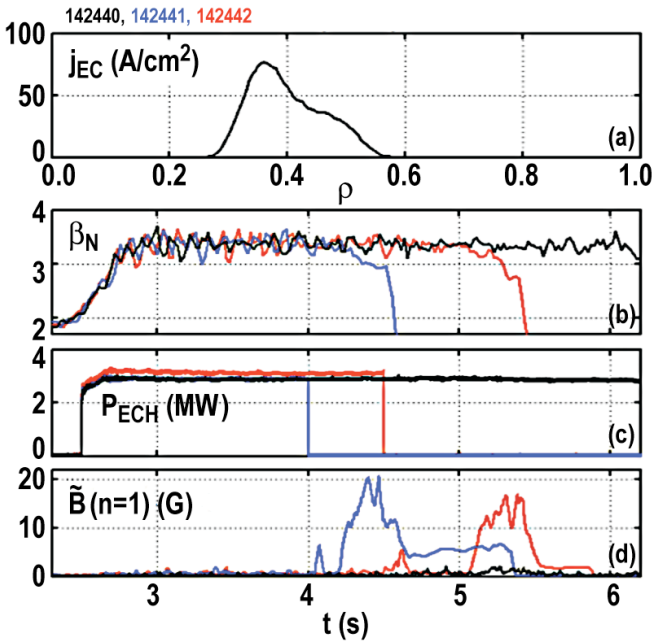

Fig. 1. Discharges from the ECCD deposition scans: (a) EC current profile, (b) β_N, (c) EC power, (d) n=1 magnetic activity.

after the EC power is turned off. The broad and relatively low power EC current profile differs substantially from the configuration used for direct stabilization of magnetic islands. Global current profile modifications are likely to be the mechanism at play, which influence directly the linear tearing index Δ' of the equilibria. At fixed q_{min} and q_{95}, a broad EC deposition ($\Delta\rho$~5–10 cm) was injected at three different positions centred at ρ~0.45, 0.55, 0.62. A sample of the results of the EC scans are represented in figure 2, where it is shown that roughly 50% of the discharges with ECCD are stable, but tearing modes are still present in some cases (with both poloidal numbers m=2 and m=3). The variability of the outcome is consistent with the modeling results obtained with the PEST3 code. One of the experimental equilibria was analysed and the tearing and interchange indexes Δ' and Γ' calculated. These show a sharp sudden increase when the plasma conditions approach the ideal MHD limit (figure 3), when an external kink instability is found by the model. When near the ideal limit (high β_N), the plasma tearing stability becomes very sensitive to small changes in the equilibrium, as seen in the experiment.

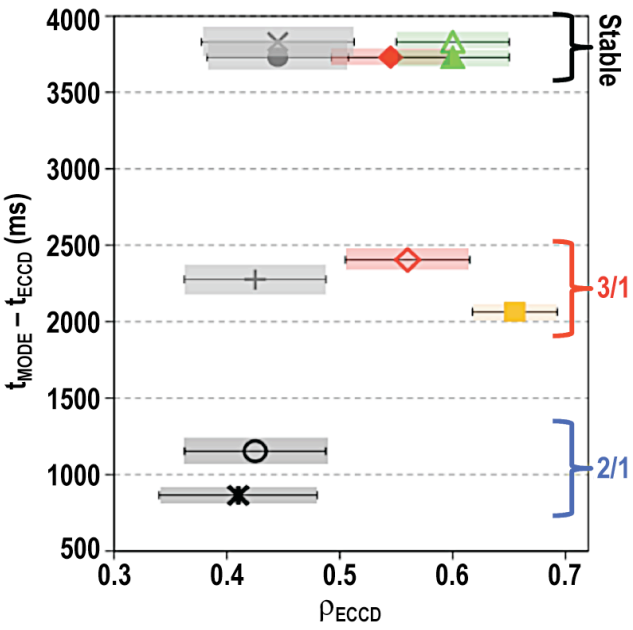

Fig. 2. Survival time of the ECCD scan discharges, against the deposition location and width. Stable discharges on the top of the plot, the type of n=1 modes are indicated on the sides.

The q profile scans indicate the path to f_{NI}=100%

The q profile scans were used to evaluate the NI current fraction and the J_{BS} magnitude and profile. Three values of q_{min} and q_{95} were used (q_{min}~1.1, 1.5, 2 and q_{95}~4.5, 5.5, 6.8) and the kinetic data were averaged over phases of both constant β_N~2.8 and maximum power. Ultimately, this allows evaluation of how transport affects the J_{BS} profile, which is a function of q, β_N and the pressure peaking factor f_p. The sum of all the changes in the equilibria show that the kinetic profiles vary sys-

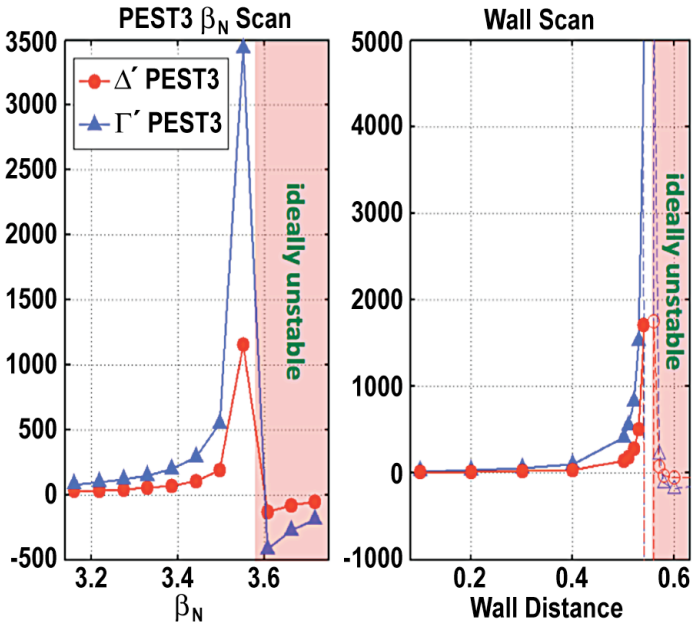

Fig. 3. PEST3 Δ' and Γ' indices, calculated for an experimental equilibrium. At fixed wall distance, β_N scan (left), at fixed pressure, wall distance scan (right).

tematically and become broader for higher q_{min} and higher β_N. At constant β_N, f_p decreases with increasing q_{min} (figure 4, blue circles), and it decreases also for higher β_N values, becoming virtually insensitive to q_{min} (red squares). The f_p trends, along with the changes in q and β_N, determine the J_{BS} profiles of the scan discharges: J_{BS} broadens with increasing q_{min}, but most importantly at high β_N it loses the central peak and becomes roughly insensitive to q_{min}. As a result, the bootstrap fraction increases with q_{95} and β_N, as expected, but it does not increase indefinitely with increasing q_{min} [1].

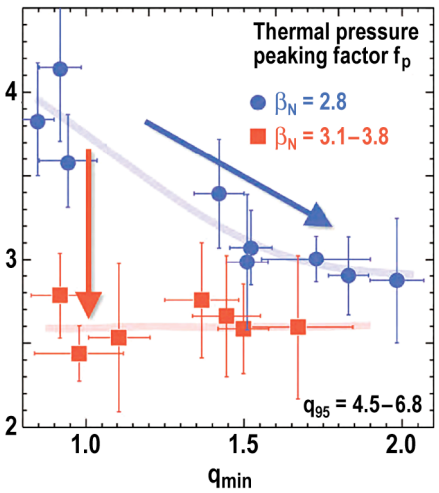

Fig. 4. Pressure peaking factor f_p for all the discharges, at fixed β_N=2.8 (blue circles) and at maximum β_N (red squares), plotted against q_{min} (all q_{95} values together).

Transport experiment and modeling

In order to investigate the reasons for the kinetic profiles variations described in the previous sections, heat transport coefficients (χ_e and χ_i) were evaluated for all the discharges, and experimental density fluctuations were collected from the Far InfraRed diagnostic. These data show that the electron and ion transport scales differently with q (figure 5): χ_i increases with q_{min} and q_{95}, while χ_e decreases with q_{min}. Electrons represent the dominant loss channel at low q_{min}, while at high q_{min} the ions dominate. The FIR data show the same trends with q for the energy available in the low wave numbers k_θ, associated with ion mode activity, which therefore is consistent with the χ_i trend. As a first step to evaluate models that could explain the results and guide the design of future experiments, the TGLF code was tested on the q scan discharges. Full radius runs were performed with and without the ExB shear and the experimental rotation profiles. The linear growth rates γ were also calculated at ρ=0.4, 0.5, 0.6, 0.7. The high wave number (k_θ) ranges vary with the q profile in a way that is not consistent with the experimental observations. Conversely, at low k_θ the γ trend can explain the growth of χ_i with q_{min}, but it contradicts the transport variation with q_{95}. In the simulations, the gradients were allowed to relax and a sensitivity study was performed to ensure that the results are not affected by systematic errors. Since the linear

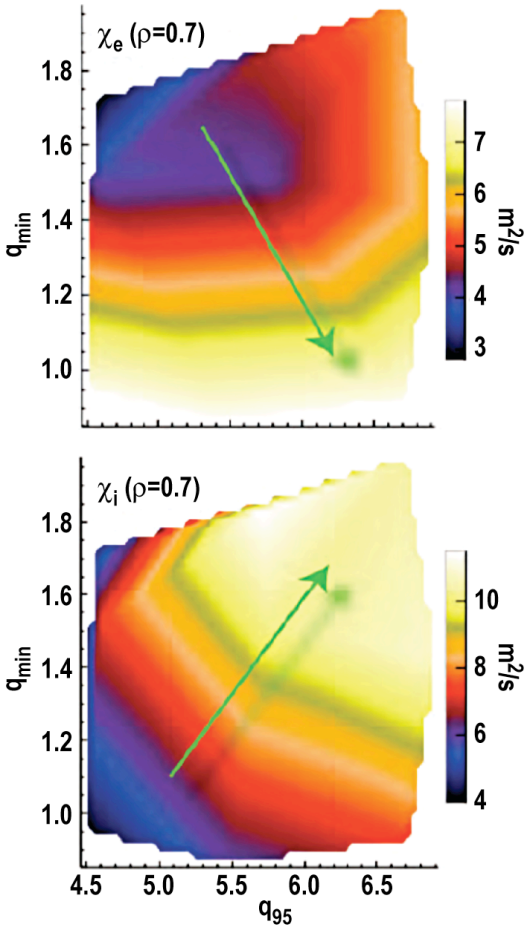

Fig. 5. Variations of χ_e and χ_i with q_{min} and q_{95}, as evaluated from the experimental data.

growth rates represent the energy available for the ion and electron transport in the plasma, these results suggest either that (i) the nonlinear saturation state must reverse the linear trends to make them follow the experimental observations, or that (ii) some physics is missing in the linear calculation [2].

Summary and conclusions

This study shows that the highest f_{NI} is reached at the highest q_{95} value, and the shape of the total J is best matched by J_{NI} at $q_{min} \geq 1.5$ (figure 6). Since the bulk of the NI current is driven on axis by the neutral beam power, reaching higher β_N levels – positive for bootstrap current production – also entails the risk of overdriving the central current profile. The same can be said about the choice of higher q_{min} configurations. These conclusions, along with the need for additional off-axis current, motivated the installation of the new tilted neutral beam line, which is currently being used to explore higher q_{min} scenarios and different current alignments. The TGLF comparison with the experimental data indicates that the linear growth rate prediction of the code do not yet correlate with the measured transport rates, and more extensive (and possibly nonlinear) work is needed to explain the physics mechanisms at play. The deposition location of J_{EC} that is attractive for tearing stability is also compatible with the position where the additional NI current is required. However, PEST3 results indicate that the approach to the ideal MHD limit makes the stability particularly sensitive to small changes in the equilibrium, and reproducibility of the results becomes an issue. For this reason, new modeling cases are being used to design equilibria with higher ideal and tearing limits.

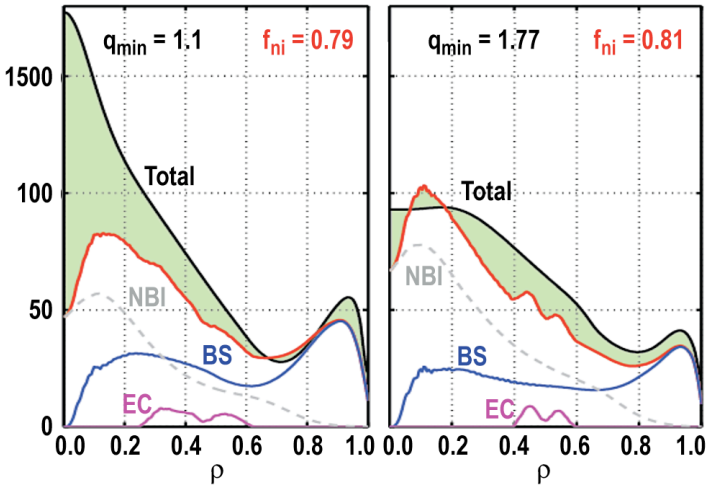

Fig. 6. Total J (black line) and alignment of the total NI current (red), neutral beam current (grey), J_{BS} (blue) and J_{EC} (purple) for the cases with lowest (left) and highest (right) q_{min}, at maximum β_N. The missing NI current is represented by the green shaded area.

Work supported in part by the US Department of Energy under DE-FC02-04ER54698, DE-AC52-07NA27344, DE-FC02-93ER54186 and DE-FG02-06ER84442.

[1] J.R. Ferron, Nucl. Fusion **51**, 063028 (2011).

[2] C.T Holcomb, "The effect of safety factor profile on transport in steady state, high performance scenarios", submitted to Nucl. Fusion 2011.